ACS SENSORS

pubs.acs.org/acssensors

Article

iHWG-MOX: A Hybrid Breath Analysis System via the Combination of Substrate-Integrated Hollow Waveguide Infrared Spectroscopy with Metal Oxide Gas Sensors

Johannes Glöckler, Carsten Jaeschke, Yusuf Kocaöz, Vjekoslav Kokoric, Erhan Tütüncü, Jan Mitrovics, and Boris Mizaikoff*

Cite This: *ACS Sens.* 2020, 5, 1033−1039

Read Online

ACCESS | Metrics & More | Article Recommendations

ABSTRACT: According to their materials and operating parameters, metal oxide (MOX) sensors respond to target gases only by a change in sensor resistance with a lack in selectivity. By the use of infrared spectroscopy, highly discriminatory information from samples at a molecular level can be obtained and the selectivity can be enhanced. A low-volume gas cell was developed for a commercially available semiconducting MOX methane gas sensor and coupled directly to a mid-infrared gas sensor based on substrate-integrated hollow waveguide (iHWG) technology combined with a Fourier transform infrared spectrometer. This study demonstrates a sensing process with combined orthogonal sensors for fast, time-resolved, and synergic detection of methane and carbon dioxide in gas samples.

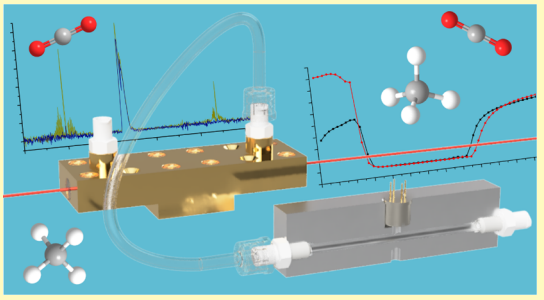

KEYWORDS: *eNose, metal oxide sensor, substrate-integrated hollow waveguide, iHWG, breath diagnostics, breath analysis*

Because physical and biochemical methods in medical monitoring and diagnostics have rapidly increased, breath analysis, as a noninvasive sensing method, became more and more important. Advances in the identification of disease biomarkers increased the interest in exhaled breath analysis for early disease detection and emerged new sensing methods.[1,2] The complex matrix of exhaled breath is predominantly a mixture of N_2, O_2, H_2O, and CO_2 along with more than 1000 volatile organic compounds (VOCs) at trace levels (ppt to ppm), which varies widely from person to person.[3] As the composition of exhaled breath corresponds to complex biochemical processes within the body, a large number of these VOCs may serve as potential biomarkers for specific diseases or metabolic disorders.[2]

Methane is the simplest hydrocarbon, and inhaling it can cause suffocation. Potential effects at low concentrations are headaches and dizziness that can be accompanied by nausea as levels increase and unconsciousness till death.[4] Methane has been identified in exhaled breath as a biomarker for colonic fermentation.[5] Furthermore, studies demonstrated that methane in exhaled breath is significantly associated with constipation in bowel patients. The detection of methane in exhaled breath could also be used as a diagnostic test for constipation and further direct the medical treatment of patients (e.g., antibiotic approach).[6] Studies have found up to 70 ppm of methane and 4−5% of CO_2 in breath samples from subjects with methane-producing colonic bacteria, which can be associated with irritable bowel syndrome.[7−9]

However, the rather minute concentrations of VOCs in the exhaled breath matrix pose a challenge to many sensing applications.[10] Gas chromatography combined with mass spectrometry (GC−MS) is an analytical method which covers a wide variety of compounds with high sensitivity and precision and is considered to be the current gold standard method in breath diagnostics.[2] Despite excellent sensitivity, GC−MS has some drawbacks including bulky dimensions, high instrumentation costs, the need for highly trained personnel, and elaborate sample preparation. Furthermore, the response time is limited and is therefore less suitable for real-time analysis and continuous monitoring.[11] Highly specialized methods for breath VOCs are selected ion flow tube mass spectrometry and proton transfer reaction mass spectrometry, both of which provide real-time analysis; hence, their availability and costs limit the common application.[2,12−14]

Consequently, ideal breath analyzers should enable real-time analysis, be inexpensive, comprise a small size, and provide inherent molecular selectivity. Excellent approaches therefore are optical methods based on infrared (IR) spectroscopy for

Received: December 24, 2019
Accepted: March 19, 2020
Published: March 19, 2020

https://dx.doi.org/10.1021/acssensors.9b02554
ACS Sens. 2020, 5, 1033−1039

direct sensing without extensive gas sample pretreatment, enabling a nondestructive, selective, sensitive, and fast detection or monitoring of molecular constituents.[15,16] A sensor system for gas-phase IR spectroscopy is composed of three optical components: the light source, the gas cell, and the detector. The mid-infrared region (MIR), as a light source, has proven to have high molecular selectivity by highly discriminative evaluation of excited vibro−rotational transitions and sensitivity at trace-level concentrations, capability to real-time monitoring, and possibility to integration and miniaturization to a compact device footprint.[2,17] Conventional multipass gas cell assemblies (e.g., white cell or Herriott cell) for IR spectroscopic investigations achieve high sensitivity through extended absorption path lengths (several tens of meters); however, these systems are usually bulky and require higher probe volume (200 mL up to several liters) and longer sample transient.[10,18]

To overcome the volume limitations of multipass cells for breath diagnostics, Fourier transform infrared spectroscopy (FTIR) in the mid-infrared spectral range was performed successfully in combination with fiber-optical hollow waveguides (HWGs) to monitor $^{13}C/^{12}C$ ratios in mouse breath samples.[19] HWGs are coated silica or glass tubes, which serve as a light conduit and simultaneously as a low-volume gas cell with a short transient time. However, their deficiency in robustness, flexibility, and compactness lead to further improvements.

A new generation of HWGs is the so-called substrate-integrated HWG (iHWG). The light-guiding channel is integrated into the solid-state material, which builds also the miniaturized gas cell, therefore improving the robustness and also allowing different geometries to enhance the optical path length (OPL) in a small device footprint. In contrast to equally robust industrial process monitoring systems (e.g., by Horiba), which enable monitoring high gas flows in harsh environments, iHWGs may also be used to analyze exceedingly small flows and, thus, minute sample volumes. This results in rapid sample transient times and, correspondingly, an improved time resolution.[17,18,20] iHWGs have nowadays evolved into a key component for a variety of gas sensing scenarios that readily combine with a wide variety of light sources.[19,21−29] To detect even traces of gas molecules, a compact combination of iHWGs with a new generation of miniaturized preconcentration devices was demonstrated for enriching and/or converting VOCs relevant in exhaled breath analysis and environmental and safety/security monitoring scenarios.[10,30,31]

Another attractive system which fulfils most of the requirements for specific routine breath analysis is the electronic nose (eNose) technology. Its advantages are portability, low cost, and noninvasiveness.[32] These systems offer a number of significant features, real-time sensor response, high sensitivity, a high variety of available sensors, and flexibility in instrument design.[33] eNose systems are based on an array of different sensors to give a specific response to a given odor. Changes in sensor signals are processed by advanced pattern recognition algorithms for the identification of fingerprints and discrimination, as the sensors have the drawback of nonselectivity.[32,34,35] Commonly used types of sensors in eNose devices are semiconducting metal oxides (MOX), conducting polymer composites, and intrinsically conducting polymers.[34]

MOX sensors gained much attention because they have been successfully used for fast and sensitive monitoring of trace amounts of environmentally important gases such as carbon monoxide and nitrogen dioxide and detection of gas leakages under atmospheric conditions.[36,37] This type of gas sensor is composed of a sensitive layer deposited on a substrate (e.g., ceramic Al_2O_3), which is provided with electrodes to measure electrical characteristics, such as conductivity. The device is heated by a built-in resistive heater, which is electrically separated through an insulating layer from the electrodes and the sensing layer, to working temperatures between 200 and 400 °C.[38]

Heating the sensing layer to working temperature increases the conductivity of the semiconductor, sensitivity, and adsorption/desorption processes on the surface. The adsorbed oxygen plays a crucial role in the sensing principle as it enables the reduction/oxidation processes of target gases.[39] At higher temperatures, oxygen adsorbs on the surface by chemisorption, therefore appearing in a charged species through electron exchange with the conduction band.[40−43]

Besides response time and sensitivity, the ability to identify a specific gas from a mixture is another performance indicator of a gas sensor.[44] However, even though MOX sensors are highly sensitive, they are seldom highly selective, as most of them give indiscriminate response to a variety of gases and show cross-sensitivity (e.g., Figaro TGS 2611-C00 methane sensor responds also to ethanol, hydrogen, and isobutane).[45] Thus, enhancing the selectivity is another important parameter during the development of MOX sensors.[36] This may be achieved for such sensors via the so-called "fluctuation-enhanced sensing" in combination with a modulation of temperature and/or ultraviolet light at the sensor surface.[46] A higher selectivity can also be achieved via sensor arrays composed of a variety of different MOX sensors.[47]

However, another drawback of MOX sensors in breath diagnostics is that they are not feasible to detect carbon dioxide (CO_2), which is a constituent of breath and besides nitrogen and water vapor, a versatile indicator for several metabolic processes.[27] Another important clinical parameter is the so-called respiratory quotient. The respiratory quotient is the ratio of produced CO_2 over consumed O_2, which can be used as an indicator for metabolized pathways within biological systems.[48] In order to determine this, the use of optical sensors is well suited.[25]

In this investigation, an approach is presented for a fast, real-time, and simultaneous detection of CH_4 and CO_2 by IR and CH_4 by MOX.

EXPERIMENTAL SECTION

The optical setup for sample flow-through measurements is schematically illustrated in Figure 1. The red line shows the optical path of IR radiation. MIR radiation emitted from the FTIR

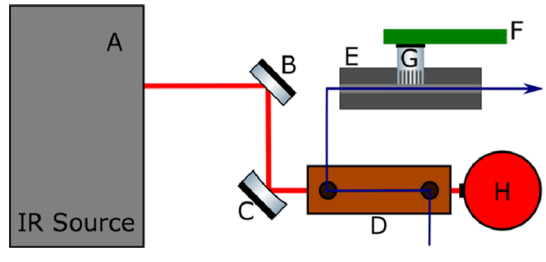

Figure 1. Schematic illustration of the optical setup for the flow-through experiments.

https://dx.doi.org/10.1021/acssensors.9b02554
ACS Sens. 2020, 5, 1033−1039

spectrometer (A) (IRcube, Bruker Optic GmbH, Ettlingen, Germany) was first reflected by a planar gold mirror (B) onto an off-axis parabolic mirror (C) (both by Janos Technology Inc., Keene, NH, USA) and focused onto the incoupling facet of a 75 mm straight-channel iHWG (D) (Research Team IABC, Ulm University). After propagating through the iHWG, emanating IR radiation from its distal end was directly focused to a liquid nitrogen-cooled mercury–cadmium–telluride (MCT) detector (H) (InfraRed Associates Inc., Stuart, FL, USA) with an active detector element area of 4 mm^2, which also matched the dimensions of the iHWG channel. Spectral interferences of ambient air constituents were avoided by encasing the whole optical setup using commercially available large low-density polyethylene polymer bags.

The TGS 2611-C00 MOX gas sensor (G) (Figaro Engineering Inc., Mino, Osaka, Japan) was pinned on the MOXstick USB interface (F) (JLM Innovation GmbH, Tübingen, Germany), inserted gastight into the MOX gas flow-through cell (E) (sensor cap sealed with one layer of Teflon tape). The MOX gas flow-through cell (gas inlet) was then connected with the iHWG (gas outlet) using a 10 cm hose of 1 mm diameter with luer-lock connections (B. Braun Melsungen AG, Melsungen, Germany). The MOX sensor was preheated 1 day prior to experiment under its circuit conditions (circuit voltage V_C = 5.0 V and heater voltage V_H = 5.0 V).

Measurement Procedure. Before each measurement, both iHWG and MOX gas flow-through cells were purged using synthetic air (20.5% O_2, 79.5% N_2, MTI IndustrieGase AG, Neu-Ulm, Germany) at a flow rate of 100 mL/min. MOX experiments and IR measurements were started simultaneously. Immediately after recording the IR background spectra, 10 repeated sample measurements were started and a defined gas mixture was set on the gas mixing system. After recording five IR spectra of the sample, the gas flow was instantly turned only to synthetic air to get the course of the purging step.

Data Acquisition. For IR data acquisition and processing, OPUS 6.5 (Bruker Optik GmbH, Ettlingen, Germany) software package was used. Each IR spectrum is recorded in the spectral range of 4000–700 cm^{-1} with a resolution of 2 cm^{-1} using a Blackman–Harris three-term apodization function and is an average of 100 scans, which correspond to 40 s. The MOX sensor signals were recorded using JLMlogSP 2.5 software (JLM Innovation GmbH, Tübingen, Germany) every 10 s. Therefore, it was possible to obtain a time-resolved methane profile for both IR and MOX measurements.

Data Evaluation. Each measurement was repeated three times, and for the MOX measurements, five different gas sensors were used. The average value was calculated from the 15 values obtained. The error is represented as the standard deviation of the measured values. For IR spectral evaluation of methane and carbon dioxide, an integration method was developed with spectral regions, whose parameters are listed in Table 1. Mean averaged values of the integrated peak area were then plotted against time. For the relation between different sample concentrations and sensor feedback, sensor resistance changes of the MOX gas sensor during sample flow-through were analyzed and six signals (which correspond to 60 s) before the purging process were picked out for data evaluation and averaged for each sample.

Table 1. Parameters for IR Spectral Evaluation

		baseline correction [cm^{-1}]	
band	integration [cm^{-1}]	region 1	region 2
CH_4 band 1	3150–2875	3550–3300	2700–2550
CH_4 band 2	1375–1225	1950–1800	1150–1000
CO_2	2390–2280	2700–2550	2200–2050

Apparatus. The iHWG (75 mm × 25 mm × 20 mm, $L \times W \times H$) used in this study (Figure 2a) was fabricated from the brass alloy substrate ($CuZn_x$). It provides an optical path length of 70 mm with a cross section of 2.1 × 2.0 mm. Both substrates were polished with commercially available diamond polishing suspensions to a mirror-like finish to obtain high surface reflectivity. To further improve reflectivity, a gold layer was galvanically deposited on the wave-guiding channel. For enhancing the adhesion between gold and the substrate and protecting brass from oxidation, an intermediate copper layer (copper layer thickness of approximately 1 μm) was applied through galvanic plating. Both ends were sealed gastight with MIR-transparent BaF_2 windows to form also a highly miniaturized gas cell, which encloses a volume of 294 μL.[17]

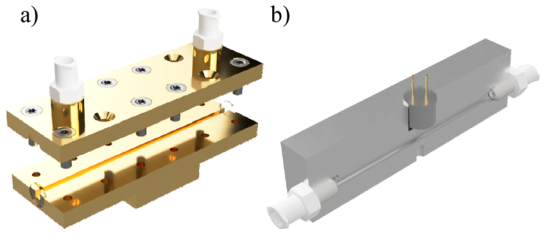

Figure 2. Cross-sectional view of (a) iHWG and the (b) MOX gas cell.

To match the compact dimensions of the iHWG (75 mm), the entire MOX gas flow-through cell was machined from the 75 × 20 × 20 mm ($L \times W \times H$) aluminum block (Figure 2b). This material provides robustness, low weight, high thermal conductivity, and high stability against oxidation. Integration of the 75 mm-long gas channel was achieved on a lathe by drilling from both sides to create a through hole with a diameter of 3 mm, resulting in an internal volume of 600 μL. On both sides of the channel, M5 female luer-lock connectors with PTFE O-rings were installed. A sensor fitting was introduced into the device on top of the surface for the standardized TO-5 (transistor outline) package followed by a small channel of 3 mm diameter to allow access from the MOX sensor to the gas channel. For further precise fitment of the sensor, a flat 0.5 mm-deep countersink with a diameter of 9.5 mm was cut for the sensor pin marker.

RESULTS AND DISCUSSION

The performance of MOX gas sensors with iHWGs were evaluated in terms of sensitivity, precision, and orthogonality.

Figure 3 shows the whole absorption spectra of a sample measurement from 100 ppm CH_4 (blue) and 1000 ppm CH_4 (ochre), both with 1000 ppm CO_2. In both samples, CO_2 can be clearly detected; however, 100 ppm CH_4 is not possible to differentiate from noise with the used setup and measurement procedure for MIR-iHWG measurements.

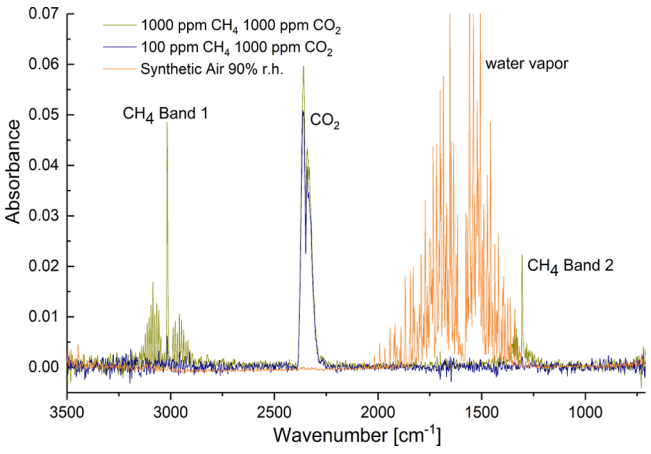

Figure 3. IR absorption spectra of 1000 and 100 ppm CH_4 with 1000 ppm CO_2 in comparison to humidified air/water vapor.

As shown in Figure 3, the selected spectral windows, summarized in Table 1, offer readily accessible absorption

https://dx.doi.org/10.1021/acssensors.9b02554
ACS Sens. 2020, 5, 1033–1039

lines. There is no overlap of the CH_4 band 1 and the CO_2 band with a potentially interfering water signal resulting from humidity. Consequently, both dry gas samples and humid samples may readily be analyzed.

In Figure 4a, methane profiles (100 and 1000 ppm) of samples with and without carbon dioxide are compared (for

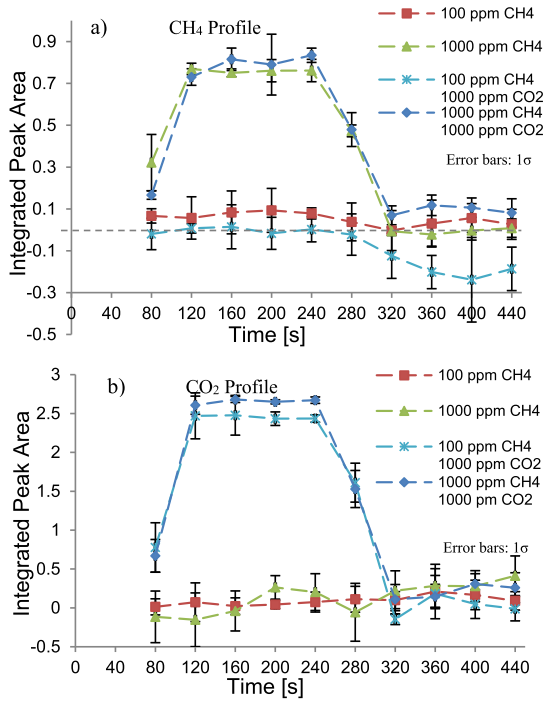

Figure 4. (a) Comparison of the CH_4 profile with and without 1000 ppm CO_2. (b) Time-resolved carbon dioxide profile of samples with and without 1000 ppm CO_2 in methane and synthetic air.

CH_4 band 1) and show the same course as CO_2 does not affect methane absorption. The same samples are compared in their carbon dioxide profile, as shown in Figure 4b. Both samples with 1000 ppm CO_2 show a high absorption between 2390 and 2280 cm^{-1}; hence, their integrated areas are equal. In the IR spectrum, it is possible to distinguish between signals as gas samples without CO_2 show no absorption in this spectral range. Therefore, the feasibility of MIR absorption spectroscopy using iHWG for selective and simultaneous detection of methane and carbon dioxide is demonstrated.

The MOX sensor was set to record one signal every 10 s, which allowed a high time-resolved tracking of the samples compared to the simultaneously started iHWG measurement (one spectrum every 40 s). Other than the IR spectrum (absorbance increases with increasing concentrations), increasing concentrations of methane cause a decrease in MOX sensor resistance. Likewise, a change in sensor response for 100 ppm CH_4 is still detectable, which can be seen in Figure 5.

Data plotted in Figure 5a show that methane has a nonlinear sensor response to sample concentration for the MOX sensor. The higher time resolution has an advantage in data processing as every 10 s a new signal is recorded, more signals can be compared with the other two measurements of the sample and not only one signal like in the iHWG experiments. Therefore, variations through timing have a lower effect for MOX measurements. For the error bars in Figure 5b, the triple standard deviation of the 15 measured values obtained by repeating a measurement three times for each of the five

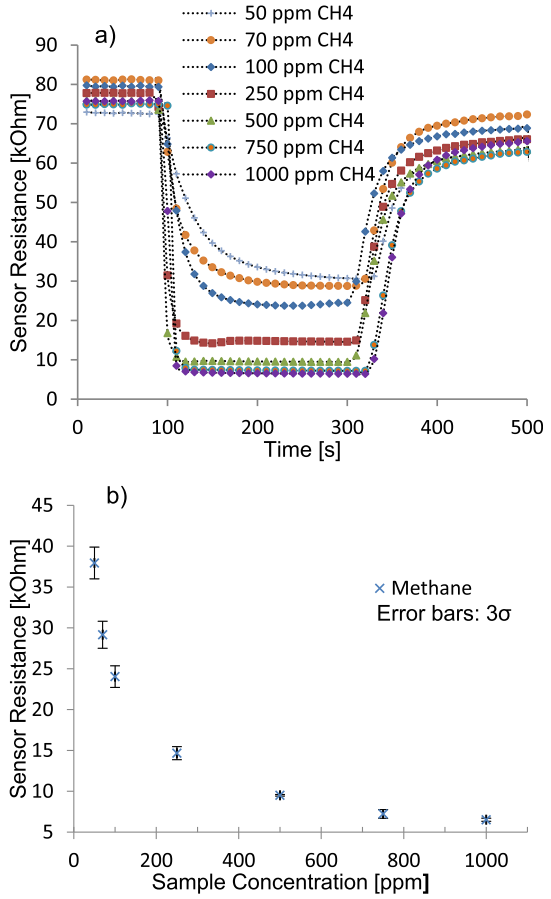

Figure 5. (a) MOX sensor resistance change during flow-through measurements. (b) $R_{s,m}$ values vs different methane sample concentrations.

investigated MOX sensors was used. Starting with the 250 ppm methane measurements, the errors become larger with lower concentrated samples. The manufacturer of the MOX sensor suggests a sensitivity for methane above 300 ppm. This could be one reason for the deviations at 100 ppm CH_4, but it is still possible to detect this low sample concentration.

The experiments were performed with and without 1000 ppm CO_2 in the methane sample. As compared in Figure 6, no

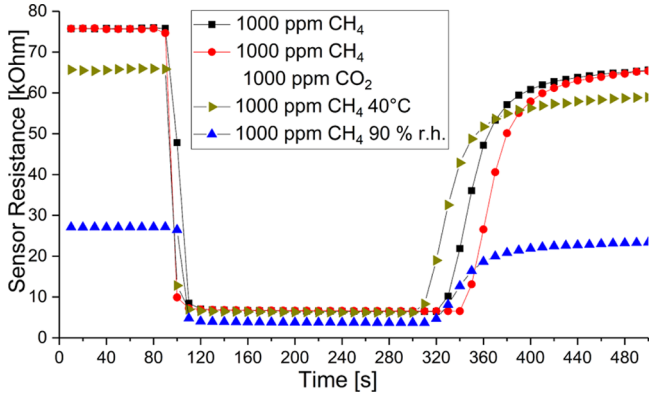

Figure 6. Trajectory of sensor resistance change during the measurement of 1000 ppm CH_4 (black), 1000 ppm CH_4 with 1000 ppm CO_2 (red), 1000 ppm CH_4 at 40 °C (gold), and 1000 ppm CH_4 at 40 °C and 90% r.h. (blue).

https://dx.doi.org/10.1021/acssensors.9b02554
ACS Sens. 2020, 5, 1033−1039

significant influence of CO_2 on the sensor signal is detected. The slight change evident for both samples is explained by the drift of the MOX sensor. Also, the presence of oxygen increases the sensor resistance and decrease the conductivity. Hence, a lower oxygen content of the sample could affect the slight decrease in sensor resistance.

In addition, data from measurements at 40 °C and at 40 °C with 90% relative humidity were displayed. Here, it can be seen that with increasing temperature, the resistance decreases slightly. In the presence of humidity, however, the resistance drops significantly more. However, this is not a major problem for possible applications in breath gas analysis as these changes in resistance are reproducible and constant for each condition.

Although a slight change in sensor resistance occurs with CO_2, the signals are nonspecific. A high sensitivity to methane gas does not mean a high selectivity of the MOX sensor. The combination of MOX with iHWG leads to a synergy effect because CO_2 and CH_4 can be differentiated in the spectrum, and performing quantitative measurements is possible.

CONCLUSIONS AND OUTLOOK

Our research shows that the combination of an iHWG with a low-volume MOX gas cell is an approach to enhance the selectivity of MOX sensors and hence their success in eNose systems for breath diagnostics with additionally gained highly discriminatory information from samples at a molecular level with optical measurements.

Highly sensitive simultaneous measurements in real time could be demonstrated for trace-level methane gas and carbon dioxide in synthetic air during flow-through experiments in real time.

The combination of these two orthogonal sensor technologies, where a physical and a chemical sensor cooperate, allows us to overcome the disadvantages of the system-inherent limitations of both sensors. This is possible because the sensors operate in time coordination and thus complement their own analytical response.

A synergic effect has been demonstrated for the use of the two sensor technologies as 100 ppm of methane was not possible to quantify in the IR measurement, but a signal change was still detectable with the MOX sensor.

This signal change, of course, is not sufficient to make a statement about the molecules present in the measured sample. Only in combination with the IR measurements, molecules can be identified, even if the IR signal is too low to make a statement about the quantitative composition of the sample.

A high time-resolved signal change (1 signal/10 s) was recorded by the MOX sensor during experiments compared to iHWG, which needed 40 s for one spectrum (100 sample scans averaged to one spectrum) and showed slight deviations, as only one spectrum could be used for evaluation. This drawback could be improved by increasing the number of sample measurements or by reducing the spectral resolution and/or the number of averaged scans for each spectrum. However, this would negatively affect the spectral quality (higher noise level) and consequently the achievable limit of detection.

The detection of CO_2 and the simple recognition of concentrations in complex gas samples are not possible with a single MOX sensor. The combination with IR measurement, which allows us to read the concentration of each molecule, provides additional possibilities to calibrate and use MOX sensors with gas samples of complex composition.

The established combination is an approach for future research in breath analysis using IR spectroscopy and MOX sensors. For measurements of exhaled breath gas samples containing humidity, all fluidic pathways have to be heated to avoid condensation. For most MOX sensors, an increased temperature and the presence of humidity do not cause a sensitivity problem because the measured resistance is only additionally lowered by these factors.

By combining both cells into one device, the dead volume should be reduced. Therefore, the setup could be extended to an MOX array, thereby forming a hybrid electronic Nose system ("iHWG-eNose") for further discriminating sensor responses to different molecules.

Instead of a simple commercial sensor, one may also integrate one or more temperature and/or UV light modulated sensors for enhanced selectivity. A combination whereby the MOX sensor and IR system modulate each other is of course also conceivable.

To employ the device in real-world breath analysis, further improvements are necessary to improve the selectivity (e.g., using filters) and increase limits of detection.

Also, further system miniaturization is imagined using other light sources [e.g., MIR quantum cascade lasers (QCLs)] and detectors [e.g., deuterated triglycine sulfate detectors (DTGS)] instead of the FTIR spectrometer and liquid nitrogen-cooled MCT detector for iHWG measurements, which would enable portable systems.

AUTHOR INFORMATION

Corresponding Author

Boris Mizaikoff − *Institute of Analytical and Bioanalytical Chemistry, Ulm University, 89081 Ulm, Germany;* orcid.org/0000-0002-5583-7962; Email: boris.mizaikoff@uni-ulm.de

Authors

Johannes Glöckler − *Institute of Analytical and Bioanalytical Chemistry, Ulm University, 89081 Ulm, Germany;* orcid.org/0000-0003-1941-2665

Carsten Jaeschke − *Institute of Analytical and Bioanalytical Chemistry, Ulm University, 89081 Ulm, Germany; JLM Innovation GmbH, 72070 Tübingen, Germany*

Yusuf Kocaöz − *Institute of Analytical and Bioanalytical Chemistry, Ulm University, 89081 Ulm, Germany*

Vjekoslav Kokoric − *Institute of Analytical and Bioanalytical Chemistry, Ulm University, 89081 Ulm, Germany*

Erhan Tütüncü − *Institute of Analytical and Bioanalytical Chemistry, Ulm University, 89081 Ulm, Germany*

Jan Mitrovics − *JLM Innovation GmbH, 72070 Tübingen, Germany*

Complete contact information is available at: https://pubs.acs.org/10.1021/acssensors.9b02554

Author Contributions

J.G. and C.J. contributed equally. J.G. and C.J. wrote the article; J.G. and Y.K. analyzed the data; Y.K. and V.K. conceived and performed the experiments; E.T. contributed infrastructure and materials; and B.M. proofread the article.

Notes

The authors declare no competing financial interest.

https://dx.doi.org/10.1021/acssensors.9b02554
ACS Sens. 2020, 5, 1033−1039

■ ACKNOWLEDGMENTS

The authors acknowledge the support of the members of the Institute of Analytical and Bioanalytical Chemistry (IABC) at Ulm University. Partial support of this study by the Deutsche Forschungsgemeinschaft (DFG) under research grant agreement GRK2203-PULMOSENS is greatly acknowledged. This work has been supported by the Horizon 2020 Framework Programme of the European Union within the VOGAS Project under project number 824986. The Machine Shop at Ulm University is thanked for support during prototype development.

■ REFERENCES

(1) Cao, W.; Duan, Y. Breath Analysis: Potential for Clinical Diagnosis and Exposure Assessment. *Clin. Chem.* **2006**, *52*, 800−811.
(2) Kim, S.-S.; Young, C.; Vidakovic, B.; Gabram-Mendola, S. G. A.; Bayer, C. W.; Mizaikoff, B. Potential and Challenges for Mid-Infrared Sensors in Breath Diagnostics. *IEEE Sens. J.* **2010**, *10*, 145−158.
(3) Phillips, M.; Herrera, J.; Krishnan, S.; Zain, M.; Greenberg, J.; Cataneo, R. N. Variation in Volatile Organic Compounds in the Breath of Normal Humans. *J. Chromatogr. B: Biomed. Sci. Appl.* **1999**, *729*, 75−88.
(4) Lawrence, N. Analytical Detection Methodologies for Methane and Related Hydrocarbons. *Talanta* **2006**, *69*, 385−392.
(5) Le Marchand, L.; Wilkens, L. R.; Harwood, P.; Cooney, R. V. Use of Breath Hydrogen and Methane as Markers of Colonic Fermentation in Epidemiologic Studies: Circadian Patterns of Excretion. *Environ. Health Perspect.* **1992**, *98*, 199−202.
(6) Kunkel, D.; Basseri, R. J.; Makhani, M. D.; Chong, K.; Chang, C.; Pimentel, M. Methane on Breath Testing Is Associated with Constipation: A Systematic Review and Meta-Analysis. *Dig. Dis. Sci.* **2011**, *56*, 1612−1618.
(7) Bernalier, A.; Lelait, M.; Rochet, V.; Grivet, J.-P.; Gibson, G. R.; Durand, M. Acetogenesis from H_2 and CO_2 by Methane- and Non-Methane-Producing Human Colonic Bacterial Communities. *FEMS Microbiol. Ecol.* **1996**, *19*, 193−202.
(8) Pimentel, M.; Chow, E. J.; Lin, H. C. Normalization of Lactulose Breath Testing Correlates with Symptom Improvement in Irritable Bowel Syndrome: A Double-Blind, Randomized, Placebo-Controlled Study. *Am. J. Gastroenterol.* **2003**, *98*, 412−419.
(9) Bond, J. H.; Engel, R. R.; Levitt, M. D. Factors Influencing Pulmonary Methane Excretion in Man. *J. Exp. Med.* **1971**, *133*, 572−588.
(10) Kokoric, V.; Wilk, A.; Mizaikoff, B. IPRECON: An Integrated Preconcentrator for the Enrichment of Volatile Organics in Exhaled Breath. *Anal. Methods* **2015**, *7*, 3664−3667.
(11) Nagle, H. T.; Gutierrez-Osuna, R.; Schiffman, S. S. The How and Why of Electronic Noses. *IEEE Spectrum* **1998**, *35*, 22−31.
(12) Turner, C.; Španěl, P.; Smith, D. A Longitudinal Study of Ammonia, Acetone and Propanol in the Exhaled Breath of 30 Subjects Using Selected Ion Flow Tube Mass Spectrometry, SIFT-MS. *Physiol. Meas.* **2006**, *27*, 321−337.
(13) Amann, A.; Poupart, G.; Telser, S.; Ledochowski, M.; Schmid, A.; Mechtcheriakov, S. Applications of Breath Gas Analysis in Medicine. *Int. J. Mass Spectrom.* **2004**, *239*, 227−233.
(14) Wang, C.; Sahay, P. Breath Analysis Using Laser Spectroscopic Techniques: Breath Biomarkers, Spectral Fingerprints, and Detection Limits. *Sensors* **2009**, *9*, 8230−8262.
(15) Hodgkinson, J.; Tatam, R. P. Optical Gas Sensing: A Review. *Meas. Sci. Technol.* **2013**, *24*, 012004.
(16) Tütüncü, E.; Kokoric, V.; Szedlak, R.; MacFarland, D.; Zederbauer, T.; Detz, H.; Andrews, A. M.; Schrenk, W.; Strasser, G.; Mizaikoff, B. Advanced Gas Sensors Based on Substrate-Integrated Hollow Waveguides and Dual-Color Ring Quantum Cascade Lasers. *Analyst* **2016**, *141*, 6202.
(17) Wilk, A.; Carter, J. C.; Chrisp, M.; Manuel, A. M.; Mirkarimi, P.; Alameda, J. B.; Mizaikoff, B. Substrate-Integrated Hollow Waveguides: A New Level of Integration in Mid-Infrared Gas Sensing. *Anal. Chem.* **2013**, *85*, 11205−11210.
(18) Fortes, P. R.; da Silveira Petruci, J. F.; Wilk, A.; Cardoso, A. A.; Raimundo, I. M., Jr; Mizaikoff, B. Optimized Design of Substrate-Integrated Hollow Waveguides for Mid-Infrared Gas Analyzers. *J. Opt.* **2014**, *16*, 094006.
(19) Wilk, A.; Seichter, F.; Kim, S.-S.; Tütüncü, E.; Mizaikoff, B.; Vogt, J. A.; Wachter, U.; Radermacher, P. Toward the Quantification of the $^{13}CO_2/^{12}CO_2$ Ratio in Exhaled Mouse Breath with Mid-Infrared Hollow Waveguide Gas Sensors. *Anal. Bioanal. Chem.* **2012**, *402*, 397−404.
(20) FTX-ONE—HORIBA https://www.horiba.com/en_en/products/detail/action/show/Product/ftx-one-1875/(accessed Dec 1, 2019).
(21) Petruci, J. F. da S.; Tütüncü, E.; Cardoso, A. A.; Mizaikoff, B. Real-Time and Simultaneous Monitoring of NO, NO_2 , and N_2O Using Substrate−Integrated Hollow Waveguides Coupled to a Compact Fourier Transform Infrared (FT-IR) Spectrometer. *Appl. Spectrosc.* **2019**, *73*, 98−103.
(22) Seichter, F.; Vogt, J.; Radermacher, P.; Mizaikoff, B. Nonlinear Calibration Transfer Based on Hierarchical Bayesian Models and Lagrange Multipliers: Error Bounds of Estimates via Monte Carlo − Markov Chain Sampling. *Anal. Chim. Acta* **2017**, *951*, 32−45.
(23) Seichter, F.; Vogt, J. A.; Wachter, U.; Radermacher, P.; Mizaikoff, B. Strategies for ^{13}C Enrichment Calculation in Fourier-Transform Infrared CO_2 Spectra Containing Spectral Overlapping and Nonlinear Abundance-Amount Relations Utilizing Response Surface Fits. *Anal. Chim. Acta* **2020**, *1095*, 48−60.
(24) Seichter, F.; Tütüncü, E.; Hagemann, L. T.; Vogt, J.; Wachter, U.; Gröger, M.; Kress, S.; Radermacher, P.; Mizaikoff, B. Online Monitoring of Carbon Dioxide and Oxygen in Exhaled Mouse Breath via Substrate-Integrated Hollow Waveguide Fourier-Transform Infrared-Luminescence Spectroscopy. *J. Breath Res.* **2018**, *12*, 036018.
(25) Tütüncü, E.; Nägele, M.; Becker, S.; Fischer, M.; Koeth, J.; Wolf, C.; Köstler, S.; Ribitsch, V.; Teuber, A.; Gröger, M.; et al. Advanced Photonic Sensors Based on Interband Cascade Lasers for Real-Time Mouse Breath Analysis. *ACS Sens.* **2018**, *3*, 1743−1749.
(26) Perez-Guaita, D.; Kokoric, V.; Wilk, A.; Garrigues, S.; Mizaikoff, B. Towards the Determination of Isoprene in Human Breath Using Substrate-Integrated Hollow Waveguide Mid-Infrared Sensors. *J. Breath Res.* **2014**, *8*, 026003.
(27) Wörle, K.; Seichter, F.; Wilk, A.; Armacost, C.; Day, T.; Godejohann, M.; Wachter, U.; Vogt, J.; Radermacher, P.; Mizaikoff, B. Breath Analysis with Broadly Tunable Quantum Cascade Lasers. *Anal. Chem.* **2013**, *85*, 2697−2702.
(28) Seichter, F.; Wilk, A.; Wörle, K.; Kim, S.-S.; Vogt, J. A.; Wachter, U.; Radermacher, P.; Mizaikoff, B. Multivariate Determination of $^{13}CO_2/\ ^{12}CO_2$ Ratios in Exhaled Mouse Breath with Mid-Infrared Hollow Waveguide Gas Sensors. *Anal. Bioanal. Chem.* **2013**, *405*, 4945−4951.
(29) Perez-Guaita, D.; Wilk, A.; Kuligowski, J.; Quintás, G.; De La Guardia, M.; Mizaikoff, B. Improving the Performance of Hollow Waveguide-Based Infrared Gas Sensors via Tailored Chemometrics. *Anal. Bioanal. Chem.* **2013**, *405*, 8223−8232.
(30) Kokoric, V.; Wissel, P. A.; Wilk, A.; Mizaikoff, B. MuciPRECON: Multichannel Preconcentrators for Portable Mid-Infrared Hydrocarbon Gas Sensors. *Anal. Methods* **2016**, *8*, 6645−6650.
(31) Petruci, J. F. d. S.; Cardoso, A. A.; Wilk, A.; Kokoric, V.; Mizaikoff, B. ICONVERT: An Integrated Device for the UV-Assisted Determination of H_2S via Mid-Infrared Gas Sensors. *Anal. Chem.* **2015**, *87*, 9580−9583.
(32) Arshak, K.; Moore, E.; Lyons, G. M.; Harris, J.; Clifford, S. A Review of Gas Sensors Employed in Electronic Nose Applications. *Sens. Rev.* **2004**, *24*, 181−198.
(33) Yadav, L.; Manjhi, J. Non-Invasive Biosensor for Diabetes Monitoring. *World J. Med. Sci.* **2014**, *11*, 82−89.

(34) Loutfi, A.; Coradeschi, S.; Mani, G. K.; Shankar, P.; Rayappan, J. B. B. Electronic Noses for Food Quality: A Review. *J. Food Eng.* **2015**, *144*, 103−111.
(35) Bochenkov, V. E.; Sergeev, G. B. Sensitivity, Selectivity, and Stability of Gas-Sensitive Metal-Oxide Nanostructures. *Metal Oxide Nanostructures and Their Applications*; American Scientific Publishers, 2010; Vol. 3, pp 31−52.
(36) Fine, G. F.; Cavanagh, L. M.; Afonja, A.; Binions, R. Metal Oxide Semi-Conductor Gas Sensors in Environmental Monitoring. *Sensors* **2010**, *10*, 5469−5502.
(37) Wang, C.; Yin, L.; Zhang, L.; Xiang, D.; Gao, R. Metal Oxide Gas Sensors: Sensitivity and Influencing Factors. *Sensors* **2010**, *10*, 2088−2106.
(38) Barsan, N.; Koziej, D.; Weimar, U. Metal Oxide-Based Gas Sensor Research: How To? *Sens. Actuators, B* **2007**, *121*, 18−35.
(39) Yamazoe, N.; Shimanoe, K. Theory of Power Laws for Semiconductor Gas Sensors. *Sens. Actuators, B* **2008**, *128*, 566−573.
(40) Yamazoe, N.; Fuchigami, J.; Kishikawa, M.; Seiyama, T. Interactions of Tin Oxide Surface with O_2, H_2O AND H_2. *Surf. Sci.* **1979**, *86*, 335−344.
(41) Barsan, N.; Weimar, U. Fundamentals of Metal Oxide Gas Sensors. *MCS 2012—14th International Meeting on Chemical Sensors*, 2012; pp 618−621.
(42) Korotcenkov, G. Metal Oxides for Solid-State Gas Sensors: What Determines Our Choice? *Mater. Sci. Eng., B* **2007**, *139*, 1−23.
(43) Taguchi, N. Gas-Detecting Device. U.S. Patent 3,631,436 A, Dec 28, 1971.
(44) Liu, X.; Cheng, S.; Liu, H.; Hu, S.; Zhang, D.; Ning, H. A Survey on Gas Sensing Technology. *Sensors* **2012**, *12*, 9635−9665.
(45) Figaro Engineering Inc. *Technical Information for TGS2611 Methane Gas Sensor*, 2017; Vol. 13.
(46) Lentka, Ł.; Smulko, J. M.; Ionescu, R.; Granqvist, C. G.; Kish, L. B. Determination of Gas Mixture Components Using Fluctuation Enhanced Sensing and the LS-SVM Regression Algorithm. *Metrol. Meas. Syst.* **2015**, *22*, 341−350.
(47) Jaeschke, C.; Glöckler, J.; El Azizi, O.; Gonzalez, O.; Padilla, M.; Mitrovics, J.; Mizaikoff, B. An Innovative Modular ENose System Based on a Unique Combination of Analog and Digital Metal Oxide Sensors. *ACS Sens.* **2019**, *4*, 2277−2281.
(48) Melzer, K.; Kayser, B.; Schutz, Y. Respiratory Quotient Evolution during Normal Pregnancy: What Nutritional or Clinical Information Can We Get out of It? *Eur. J. Obstet. Gynecol. Reprod. Biol.* **2014**, *176*, 5−9.

https://dx.doi.org/10.1021/acssensors.9b02554
ACS Sens. 2020, 5, 1033−1039